A FUNDAMENTAL APPROACH TO UNDERSTAND THE RELATIONSHIP BETWEEN TOP COAT STRUCTURE AND PAPER PERFORMANCE

Z. Richard Zhang, Roger W. Wygant, and Anthony V. Lyons
IMERYS Pigments and Additives Group
618 Kaolin Road
Sandersville, GA 31082

ABSTRACT

Profit improvement for coated freesheet and coated board will require higher efficiency or new markets. Capital investment is scarce for obtaining increases in efficiency. New markets will require improvements in optical and printing properties. The work presented here investigates how the top coating structure can be modified to enhance these properties through proper choices of blends of kaolin and calcium carbonate pigments while reducing production costs. Ultrafine and engineered kaolins were used in blends with natural and engineered ground calcium carbonates as well as with precipitated calcium carbonates. The blend ratios used included both kaolin dominated and carbonate dominated formulations. Structural parameters measured include coating pore size and volume, macroscopic and microscopic topography and coating surface voidage via goniophotometric effective index of refraction measurement. Strong relationships have been identified between optical and printing properties and these structural parameters. These conceptual relationships can be used to optimize top coating layer performance for improved printability and optics for multi-coated freesheet and woodfree grades as well as for high brightness coated board.

INTRODUCTION

The paper industry is going through some very dramatic changes. With each announcement about a new merger comes the realization that our industry has become a truly global market place. In a global market obtaining higher efficiency or opening new markets is the name of the game. In North America efficiency improvements will not come from a scarce pool of capital resources. Instead they will come from improvements in raw material costs of production. There are plenty of opportunities for improvement since expensive pigments like TiO_2 and plastic pigment are used at higher rates in North America than in the global market as a whole. What is globally true is that profit margin improvement will need to come from the generation of new market opportunities and differentiation.

In the coated freesheet and woodfree market place there are several areas of possible differentiation. These are in improvements in optics, shifts in shade to bluer and whiter, improved printability and reduced basis weights. For coated freesheet applications obtaining high levels of sheet gloss, a bluer and whiter shade, high levels in print gloss with no reduction in opacity is a difficult problem to solve especially when there are pressures to obtain a reduction in operating expenses. This can be made even more complex by adding the requirement that the basis weight be reduced without affecting the efficiency of the printer and maintaining good surface coverage. As an example it is quite common to make the shift to bluer and whiter shades by the use of higher levels of calcium carbonate pigments. Most often this leads to reduced opacity, reduced gloss, and a reduction in print gloss. This paper will show that optimization of the top coat through the use of the right pigment combinations can lead to improvements in these properties while maintaining or reducing a coated woodfree or freesheet mill's current cost structure.

In coated board applications these new marketing efforts focus on such areas as coated bleached board for flexographic containerboard, fine paper cover grades, and ultra-high end folding carton (traditionally European) grades. A primary route taken by several coated SBS producers to develop tonnage in these end uses involves producing higher brightness grades. The basic shift to higher carbonate levels in SBS coatings has been used to raise brightness, along with more traditional approaches such as TiO_2 usage. New binder systems have also come into widespread use, based on styrene acrylic copolymers. Fresh challenges in an alkaline versus an acid wet end face the coated SBS market with an increase in coating carbonate levels.

Pigment suppliers have rallied to these challenges with new options in engineered pigments, both kaolins and carbonates, which improve coating performance while reducing overall costs. The challenge is to know how to get coating structure that yields higher brightness, improved coverage and better printability. This study uses coated board formulations and base stock to develop and demonstrate the relationships between structure and performance. The principles developed will apply to coated freesheet and woodfree applications, especially heavier weight grades like cover stock.

THEORETICAL CONSIDERATIONS

The ability to control the particle size distribution, along with the particle shape factor, for all of the pigments used in a coating, all other things being equal, should yield better control of coating structure and hence the key performance parameters of brightness and printability. The dominant mechanism for high sheet brightness is light scattering, which is determined by pore size and volume in the coating. Mercury intrusion porosimetry provides measurements of pore radius and volume that correlate well to optical scatter, among other properties. The surface pores of a coating are believed to be responsible for ink set rate and K&N ink receptivity. Laser goniophotometry can measure glossing properties independently of the index of refraction change upon printing. However, goniophotometry can also be used to measure the effective index of refraction of a surface, a measure of surface pore volume. Other techniques, such as diamond stylus profilometry and atomic force microscopy can differentiate the macroscopic and microscopic contributions to surface roughness. These types of information are all critical for understanding relationships between coating structure and performance.

Mercury Intrusion Porosimetry

Mercury intrusion porosimeter measurement of paper coating pore spectra has been shown to correlate well to a variety of coating performance attributes [1 - 4]. Pore radius has a profound effect on optical scatter and a strong influence on capillary imbibition forces [5]. Pore volume is indicative of the bulking nature of coatings and thus the ability of a coating to hide the macroscopic roughness of the basestock. However, interpretation of pore spectra is a nontrivial exercise. There are a variety of artifacts that can influence results, particularly related to system compressibility and basestock porosity. Probably the best way to minimize these artifacts is to subtract a pore spectrum of the basestock from that of the coated sheet. This is the method that was used here.

When a basestock pore spectrum is subtracted from a coated sheet pore spectrum, artifacts related to system compressibility should be minimized. However, another 'artifact' that arises is negative pore space. This is due to basestock pores that have been filled by the coating material. Fortunately, basestock pores are typically much larger than pores within coating layers, at least for most packaging, printing and writing grades. Thus, the spectrum subtraction technique will typically yield a spectrum showing a positive space coating pore volume peak at radii in the order of 0.1 μm and a negative space filled basestock pore volume peak at larger radii, in the order of 1.0 μm.

Laser Goniophotometry

Goniophotometer is Greek for 'angle of light measurer'. In this type of measurement a laser beam is reflected off a surface and the angular intensity distribution of the specularly reflected light is measured. The measurement device uses a red HeNe laser with a wavelength of 632.8 nm and a beam diameter of 0.8 mm. This beam is normally used at an incidence angle of 75° from the surface normal for direct comparison to 75° TAPPI gloss measurements. At this incidence angle, the laser illuminates an elliptical spot on the paper surface with major and minor axis lengths of about 3 mm and 0.8 mm. The detector angular resolution is 0.25°, sufficient to resolve the information limiting laser speckle pattern. Thus, as much sample related information as can be conveyed by the laser light is captured. Note that typical human visual angular resolution varies between 0.1° and 0.01°.

Although a wide variety of statistics can be calculated from the image of the reflected laser, the most easily understood characterization is of the width of the reflected peak. The shape of the peak is approximately a Gaussian of the form,

$$\mathbf{I(\theta) = A\ exp[-((\theta - \theta_0)/\sigma_\theta)^2]} \qquad \textbf{(1)}$$

where A is related to the reflectivity of the surface, θ is the detector angle, θ_0 is the center angle of the specular reflection peak and σ_θ is the standard deviation of the Gaussian peak. The standard deviation can be found using a least squares regression algorithm. Note that this peak width is strictly dependent upon the topography of the surface and is independent of the index of refraction of a surface.

Although the goniophotometer peak width is independent of the index of refraction, the intensity of the specular peak depends explicitly upon the index of refraction. Because of this, it is possible to measure the effective index of refraction of a surface. In order to do this, it is necessary to conduct measurements on the same spot, without moving the sample, with different polarization states of the laser. The ratio of the intensities with polarization parallel to the plane of incidence (defined by the normal to the surface and the incident beam) to intensities with polarization perpendicular to that plane is used to calculate the effective index of refraction. The equation for this is,

$$\mathbf{n = \sin\theta\, [1 + \tan^2\theta\, (1 - \rho)^2 / (1 + \rho)^2]^{1/2}} \qquad \mathbf{(2)}$$

where,

$$\rho = (\mathbf{R}_{\parallel} / \mathbf{R}_{\perp})^{1/2} \qquad \mathbf{(3)}$$

and $\mathbf{R}_{\parallel}$ and $\mathbf{R}_{\perp}$ are the reflection intensities parallel and perpendicular to the plane of incidence. In general, unless TiO_2 levels are being manipulated, there is very little change in the index of refraction of the solid phase of a paper coating. This is due to the fact that kaolin, calcium carbonate and binders all have very similar indices of refraction. Thus, any measured changes in the effective index of refraction of a surface are due primarily to variation of the amount of void space in the coating structure. If the solid phase component indices of refraction are known accurately, it is possible to calculate the percent void volume at a surface assuming linear combinations. One other important point about goniophotometric index of refraction measurements is that this technique is only responsive to the top 1 µm or so of the surface. This is because this is about the maximum depth of penetration of the exponentially decaying evanescent waves of the specularly reflected laser beam. Thus, this technique responds primarily to the porosity at the very surface of the coating. This is in contrast to mercury porosimetry, which measures the porosity within the entire bulk of a sample [4 - 6].

Topography

In the research presented here, three different devices have been used to measure the roughness and topography of the coated paper surfaces. These included a Parker Print-Surf, the IMERYS Paperscape (a diamond stylus profilometer) and an Atomic Force Microscope (AFM). AFM measurements were done using a Digital Instruments Nanoscope III in a non-contact tapping mode. In this mode, the AFM probe tip is oscillated above the sample surface such that the amplitude of the oscillation is influenced by the proximity to the surface. The sample is moved vertically to maintain a constant oscillation amplitude, thus providing topographic information. The Parker Print-Surf, blowing air between the paper surface and a metal land, provides only a roughness number. Both the Paperscape and AFM provide topographical maps from which a wide variety of statistics can be calculated. Particular statistics discussed in this paper include the RMS roughness and the slope. The slope has been calculated as the average magnitude of the surface gradient, calculated using a 4-neighborhood operator on the topographical image.

There are significant differences in lateral measurement bandwidths of these instruments. The Parker is responsive primarily to roughness with lateral scales similar to the width of its metal land, approximately 50 µm. The Paperscape has a 1 mil (25.4 µm) diameter spherical tip at the end of a 90° included angle conical stylus. Scans run on samples were 1 mm in size, with an 8 µm step between points. Thus, the lateral bandwidth of roughness features that the Paperscape was responding to was from about 20 µm to 500 µm. The AFM measured 10 µm square spot sizes with 512 points in each dimension, for a step size of 0.0195 µm. Thus, it had a bandwidth from about 40 nm to 5 µm.

EXPERIMENTAL

A coating study was conducted with a laboratory coater, the Helicoater 2000, using a pre-coated SBS sheet that had a substance weight of 167 gsm, a caliper of 0.2 mm and a PPS roughness of 2.9 µm. The sheet brightness was 80.5 (ISO) and the opacity was 98.1. A range of novel pigments were used including fine #1 kaolin, engineered kaolin, standard fine GCC (ground calcium carbonate), engineered GCC, ultrafine glossing GCC and coating PCCs (precipitated calcium carbonates). Both high clay and high carbonate based formulations were tried with a common binder system at the typically higher binder levels demanded in coated SBS. Generic details of the coating formulations are provided in **Table I** below, while the identities are given in Appendix A. The coating colors were applied to the base at four different coat weights and the target coat weight was 12 g/m^2. The coater speed was kept as a constant of 400 m/min. The coated sheets were then calendered using a Beloit 750 lab calender at equal calendering conditions (150°F, 300 PLI,25 fpm and 2 nips).

Laboratory analysis of the coated boards consisted of standard testing for physical and optical properties, along with coating surface and structure measurements using various techniques. The pore structure of the coated boards whose coat weights were closest to the target coat weight was analyzed using mercury porosimetry. These samples were also analyzed with Paperscape diamond stylus profilometry and atomic force microscopy (AFM) to measure surface smoothness on both macroscopic and microscopic scales. Goniophotometry was applied on the same samples to highlight the gloss benefits of fine #1 kaolin and provide information about the particle alignment on the surface for the different pigments used. Printing of the board samples was conducted on a Prufbau with standard offset black ink to a density of 1.65. Ink on paper tack development was determined using an IMERYS internally developed method [7].

Coatings	A	B	C	D	E	F	G	H	I	J	K
Kaolin A	60	60	60	60	40	40	0	0	0	0	0
Kaolin B	0	0	0	0	0	0	60	60	60	60	60
GCC A	40	0	0	0	0	0	40	0	0	0	0
GCC B	0	40	0	0	0	0	0	40	0	0	0
GCC C	0	0	0	0	0	0	0	0	0	0	40
PCC A	0	0	40	0	60	0	0	0	40	0	0
PCC B	0	0	0	40	0	60	0	0	0	40	0
Latex, pph	16	16	16	16	16	16	16	16	16	16	16
Protein, pph	1.5	1.5	1.5	1.5	1.5	1.5	1.5	1.5	1.5	1.5	1.5

Table I. Generic coating formulation information.

RESULTS

<u>*Brightness, Color and Opacity*</u>

The results of brightness, color and opacity measurements are presented in **Table II** below. The data reported are interpolated at the target coat weight of 12 g/m^2 from a range of coatweights. **Figure 1**, showing brightness and opacity, demonstrates some interesting differences. In coatings A through D, with Kaolin A, brightness increases while opacity decreases, albeit the opacities are in the same range within the error quoted. Thus, it may be deduced that the changes are due primarily to decreasing optical absorptivity of the coating pigments. Coatings E and F have the same pigments as coatings C and D, but at different clay/carbonate ratios. Increases in both brightness and opacity from C to E and D to F must then be due to increased optical scatter. Coatings G through K, with Kaolin B, do not show inverse trends in brightness versus opacity that might be equated with changes in absorptivity. Rather, there are changes where brightness and opacity move together, indicating changes in scatter. These types of trends are duplicated in Hunter L, a and b, consistent with the hypothetical changes in the scatter and absorption.

Coatings		A	B	C	D	E	F	G	H	I	J	K
Brightness	Mean	80.1	80.3	80.5	80.7	81.2	81.3	80.8	81.4	81.5	81.5	81.5
	Std.Err.	0.1	0.1	0.1	0.1	0.1	0.1	0.1	0.1	0.1	0.1	0.1
Opacity	Mean	98.4	98.4	98.4	98.2	98.5	98.3	98.4	98.5	98.5	98.4	98.5
	Std.Err.	0.1	0.1	0.1	0.3	0.0	0.1	0.1	0.1	0.1	0.1	0.1
Hunter L	Mean	91.43	91.59	91.62	91.70	91.98	91.90	91.90	92.04	92.10	92.07	92.17
	Std.Err.	0.03	0.03	0.03	0.04	0.03	0.03	0.04	0.04	0.04	0.04	0.06
Hunter a	Mean	-0.34	-0.30	-0.33	-0.30	-0.26	-0.22	-0.34	-0.24	-0.25	-0.25	-0.26
	Std.Err.	0.01	0.01	0.01	0.01	0.01	0.01	0.01	0.01	0.01	0.01	0.01
Hunter b	Mean	2.96	2.94	2.88	2.77	2.80	2.58	3.02	2.79	2.80	2.70	2.82
	Std.Err.	0.01	0.01	0.01	0.01	0.01	0.02	0.02	0.01	0.02	0.03	0.02

Table II. Rightness, opacity and color data (interpolated at target coat weight of 12 g/m^2).

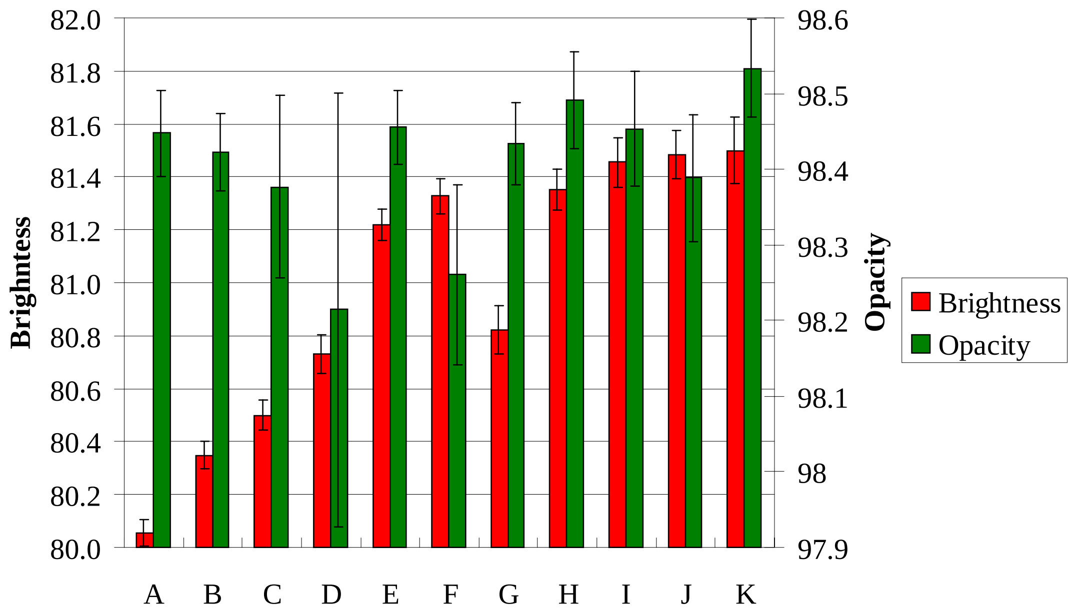

Figure 1. Brightness and opacity.

Gloss

Gloss data are presented in **Table III** and **Figures 2** and **3** below. Data presented include TAPPI 75° gloss measurements as well as goniophotometer peak widths. Figure 2 shows both sheet and print gloss, although on separate scales. It can be seen that print gloss does not duplicate the trends in sheet gloss. Figure 3 shows delta gloss as well as the change in goniophotometer peak width upon printing. While the delta glosses are all strongly positive, about half the changes in goniophotometer peaks widths are negative while the other half are positive. It should be noted that a positive change in peak width corresponds to a broadening of the peak, indicating greater sheet roughness after printing. It is noticed that in three separate comparisons of the PCCs (C vs.

D, E vs. F and I vs. J), PCC A always has a larger delta gloss and a narrower goniophotometer delta peak width than PCC B. Some of these different trends in gloss and goniophotometry changes upon printing do not appear consistent, but will be explained in terms of coating structure in the Discussion section below.

Coatings		A	B	C	D	E	F	G	H	I	J	K
75^0 Sheet Gloss	Mean	69.4	72.6	74.4	74.8	70.2	72.6	60.1	64.3	66.6	67.3	65.2
	Std.Err.	0.9	0.4	1.0	0.8	0.4	0.6	1.0	1.1	1.1	1.6	1.0
75^0 Print Gloss	Mean	94.4	97.3	97.3	95.6	97.2	96.0	92.3	96.4	96.2	95.8	95.3
	Std.Err.	1.0	0.5	0.7	1.0	0.6	0.7	0.7	0.9	0.9	1.1	0.8
75^0 Delta Gloss	Mean	25.0	24.7	22.9	20.8	27.0	23.4	32.2	32.1	29.6	28.5	30.1
	Std.Err.	1.3	0.7	1.2	1.3	0.7	0.9	1.3	1.4	1.4	1.9	1.2
Coatweight	(g/m^2)	12.1	11.8	11.6	12.8	12.1	11.3	11.4	11.7	12.8	12.2	10.7
Sheet Gonio	Mean	1.42	1.30	1.76	1.40	1.58	1.42	1.59	1.56	1.62	1.52	1.87
Peak Width (^{0})	Std.Err.	0.03	0.07	0.04	0.02	0.03	0.05	0.06	0.03	0.05	0.04	0.05
Print Gonio	Mean	1.38	1.60	1.66	1.51	1.55	1.63	1.47	1.63	1.61	1.68	1.82
Peak Width (^{0})	Std.Err.	0.09	0.04	0.06	0.05	0.09	0.07	0.06	0.06	0.05	0.03	0.05
Delta Gonio	Mean	-0.04	0.30	-0.10	0.11	-0.03	0.21	-0.12	0.07	0.00	0.16	-0.04
Peak Width (^{0})	Std.Err.	0.09	0.08	0.07	0.05	0.10	0.09	0.09	0.07	0.07	0.05	0.07

Table III. Gloss (interpolated at 12 g/m^2) and goniophotometry.

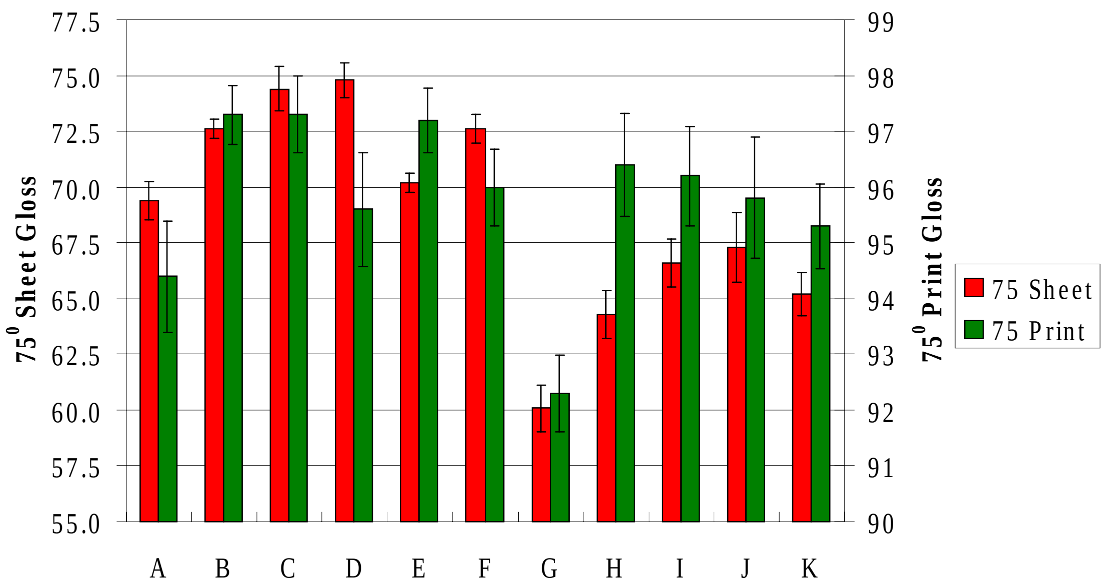

Figure 2. TAPPI 75° sheet and print gloss.

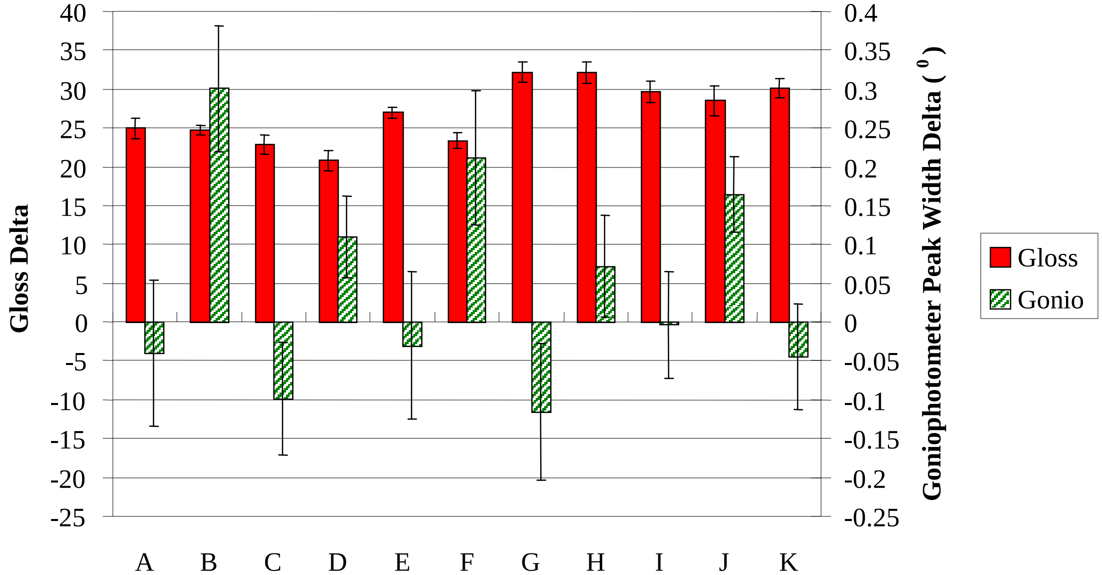

Figure 3. delta gloss and goniophotometry.

Physical Properties

Physical property measurement results except surface smoothness are presented in **Table IV** and **Figures 4** and **5** below. The effective index of refraction was measured using polarized light goniophotometry. As said before, this technique is responsive only to the top one-micron or so of the coating, the approximate depth of penetration of the evanescent waves of the specularly reflected light. Thus, it is a measure only of the surface voids. It should be mentioned that the unit of pore volume in Table IV is cc per kilogram of coated board. Figure 4 shows coating pore volume and radius measured with a mercury porosimeter, which is responsive to the entire volume of the coatings. The data shows gross differences between the kaolins used in the coatings as well as some highly significant effects of the PCCs. There is a clear distinction in the refractive index data between formulations using GCC (A, B, G, H and K) and those using PCC (C, D, E, F, I and J). These trends, present in both the refractive index and porosimeter data, will help to explain how the coating structure changes with pigmentation and how those changes affect other properties. Figure 5 presents initial ink tack slope data and the integral under the entire ink tack curve. There appear to be some relationships between the ink tack data and the various voidage measurements. These will be addressed in the Discussion section below.

Coatings		A	B	C	D	E	F	G	H	I	J	K
IGT Dry Pick	Mean	79	84	92	79	97	97	103	99	97	91	100
	Std.Err.	10	12	5	15	2	3	8	19	14	4	6
K&N Brightness	Mean	7.3	9.3	10.2	12.0	10.7	13.3	11.6	12.8	13.4	14.0	10.7
Loss	Std.Err.	0.6	0.2	0.3	1.3	0.4	0.5	0.3	0.4	1.0	1.4	0.5
Coatweight	(g/m^2)	12.1	11.8	11.6	12.8	12.1	11.3	11.4	11.7	12.8	12.2	10.7
Refractive Index	Mean	1.32	1.32	1.26	1.24	1.27	1.26	1.34	1.31	1.28	1.28	1.32
	Std.Err.	0.01	0.02	0.02	0.01	0.02	0.01	0.02	0.01	0.01	0.01	0.01
Pore Volume	(cc/kg)	8.5	7.8	6.8	12.9	7.3	8.8	6.0	4.0	4.0	9.5	4.9
Pore Radius	(nm)	24	31	36	33	40	38	63	60	69	64	50
Ink Tack Slope	(N/s)	0.0353	0.064	0.054	0.025	0.015	0.022	0.026	0.18	0.015	0.027	0.038
Tack Integral	(Ns)	142	164	145	103	140	124	219	200	204	164	202

Table IV. Physical properties (pick and K&N interpolated to 12 g/m^2).

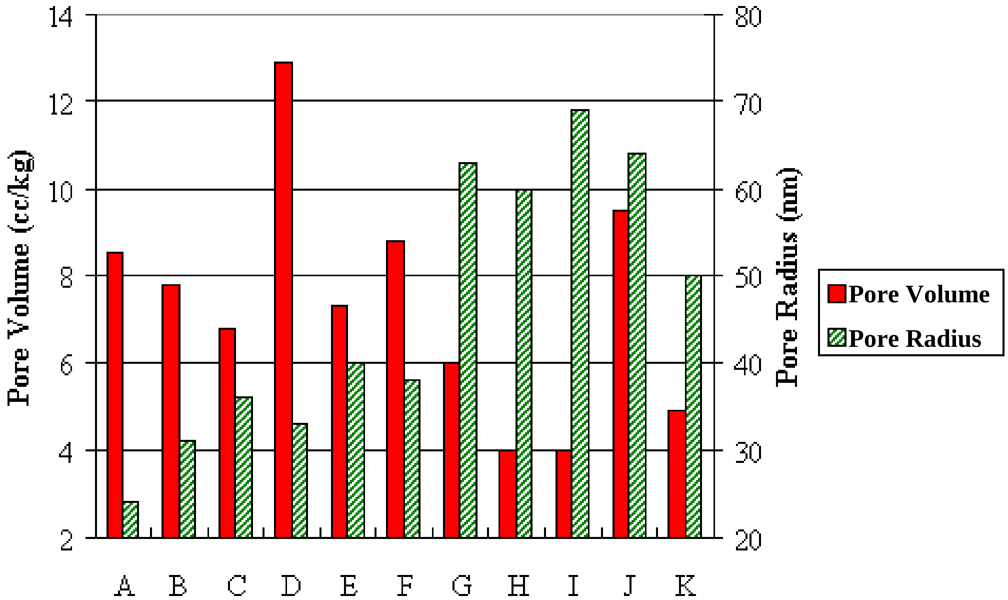

Figure 4. Coating pore radius and volume via mercury porosimetry.

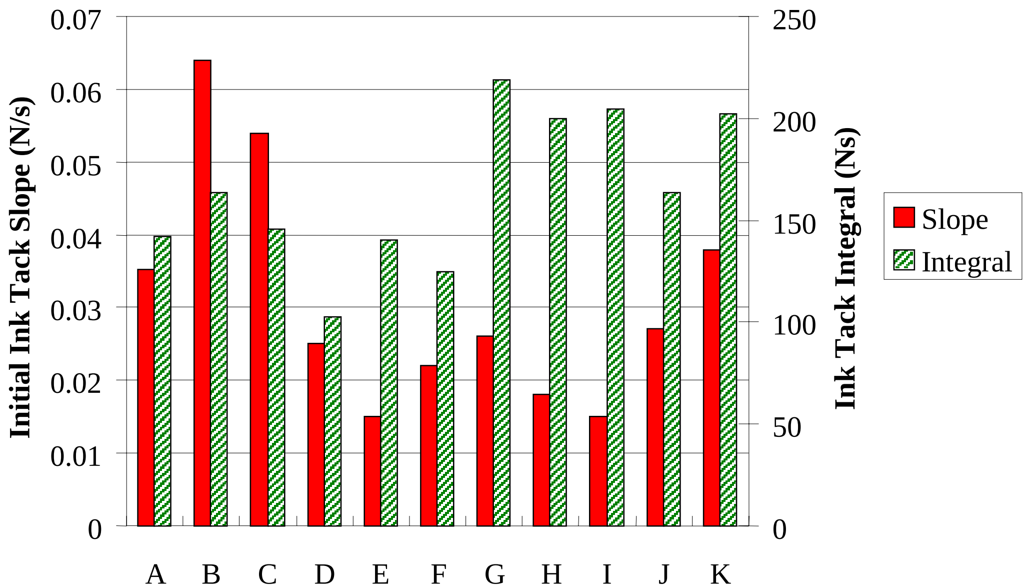

Figure 5. Ink tack slope and integral.

<u>*Surface Roughness*</u>

Surface roughness data are presented in **Table V** and **Figures 6** and **7**. Figure 6 shows roughness data from Parker Print-Surf S10 measurements, from Paperscape diamond stylus profilometry and from atomic force microscopy (AFM). Variations in the trends seen with these different instruments can be explained by the different bandwidths of the instruments. A Parker Print-Surf measures a narrow bandwidth of roughness in the neighborhood of 50 μm. The Paperscape is responsive to features between about 20 and 500 μm. The AFM gives a bandwidth between 40 nm and 5 μm. Figure 7 displays average slopes from Paperscape and AFM scans. This shows significant differences between macro and micro topography, which can be related to pigmentation and coating structure.

Coatings			A	B	C	D	E	F	G	H	I	J	K
Parker	Roughness	Mean	0.83	0.90	0.89	0.88	0.94	0.79	0.96	0.90	0.92	0.76	0.91
Print-Surf	(μm)	Std.Err.	0.07	0.07	0.06	0.05	0.08	0.06	0.07	0.06	0.06	0.05	0.06
Coatweight	(g/m^2)		12.1	11.8	11.6	12.8	12.1	11.3	11.4	11.7	12.8	12.2	10.7
Paperscape	Roughness	Mean	0.72	0.68	0.80	0.53	0.84	0.84	0.78	1.00	0.84	0.81	0.80
	(μm)	Std.Err.	0.08	0.04	0.07	0.05	0.10	0.04	0.11	0.23	0.13	0.06	0.08
	Slope (^{0})	Mean	4.9	4.3	4.9	3.5	5.1	5.1	5.0	4.4	4.9	3.7	5.1
		Std.Err.	0.5	0.1	0.1	0.3	0.4	0.4	0.2	0.9	0.5	0.6	0.3
Atomic	Roughness	Mean	0.060	0.077	0.065	0.058	0.082	0.071	0.095	0.110	0.108	0.098	0.088
Force	(μm)	Std.Err.	0.011	0.008	0.004	0.005	0.005	0.010	0.013	0.011	0.013	0.007	0.006
Microscope	Slope (^{0})	Mean	22	29	30	28	32	30	27	32	32	31	30
		Std.Err.	4	1	1	1	2	2	2	3	3	2	1

Table V. Surface roughness data (PPS interpolated to 12 g/m^2).

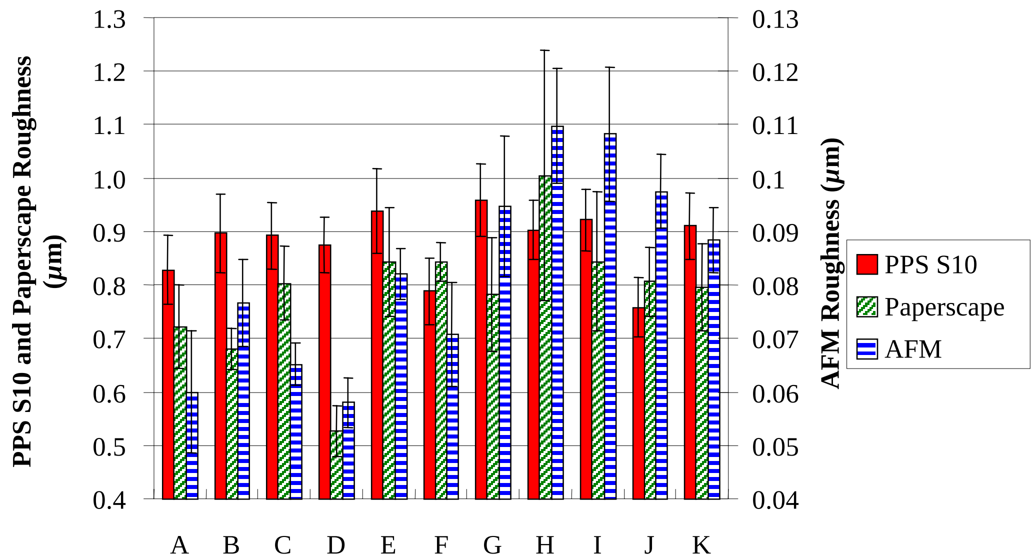

Figure 6. Parker print-surf, paperscape and atomic force microscope RMS roughness.

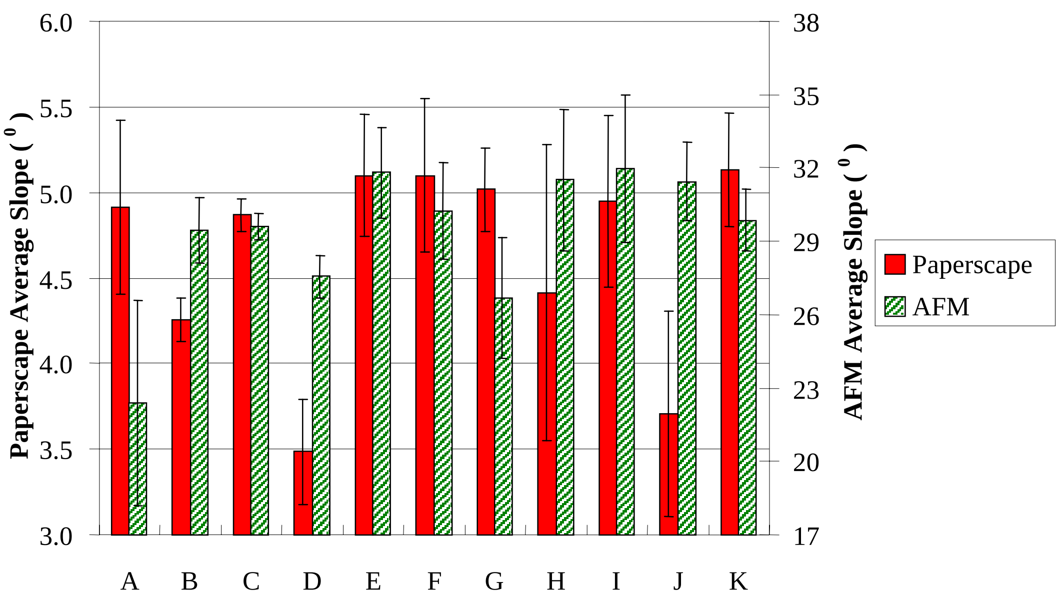

Figure 7. Paperscape and atomic force microscope average slope.

DISCUSSION

As addressed before, sheet brightness is one of the key properties for high quality SBS paperboard and coated freesheet/woodfree. It is demonstrated in the present study that sheet brightness is influenced by coating structure. **Figure 8** shows a generic trend that the sheet brightness increases as the pore size increases for the high clay based formulations. The fine #1 kaolin and the engineered kaolin have similar pigment brightness, but have a different particle shape, mean size and size distribution width. Coating with engineered kaolin results in a structure having a large average pore radius, which enhances light scatter and gives high sheet brightness. The discrepancy of the data points from the fitted line is due to the differences in pigment brightness among the carbonates used and the differences of the pore volume generated. The results for fine #1 kaolin/coating PCC based high carbonate formulations are also shown in Figure 8 as references (see also Table IV). It is clear that the high carbonate based coatings have large pore radii that enhance light scatter.

Figure 9 shows that fine #1 kaolin based formulations have advantages in achieving sheet gloss. This is because the coating was applied to a precoated base whose surface was relatively smooth and the microscopic smoothness, rather than macroscopic smoothness, prevailed in this situation. It should be mentioned that a proper choice of the carbonates in the fine #1 kaolin based formulations could yield a coated sheet with good sheet brightness as well as high sheet gloss. Glossing GCC and PCC are good candidates in this regard because they are finer than the standard GCC. Furthermore, fine #1 kaolin used in the present work allows a higher level of carbonate to be used in the formulations for higher sheet brightness without losing sheet gloss (see also Tables II & III for colors E &F).

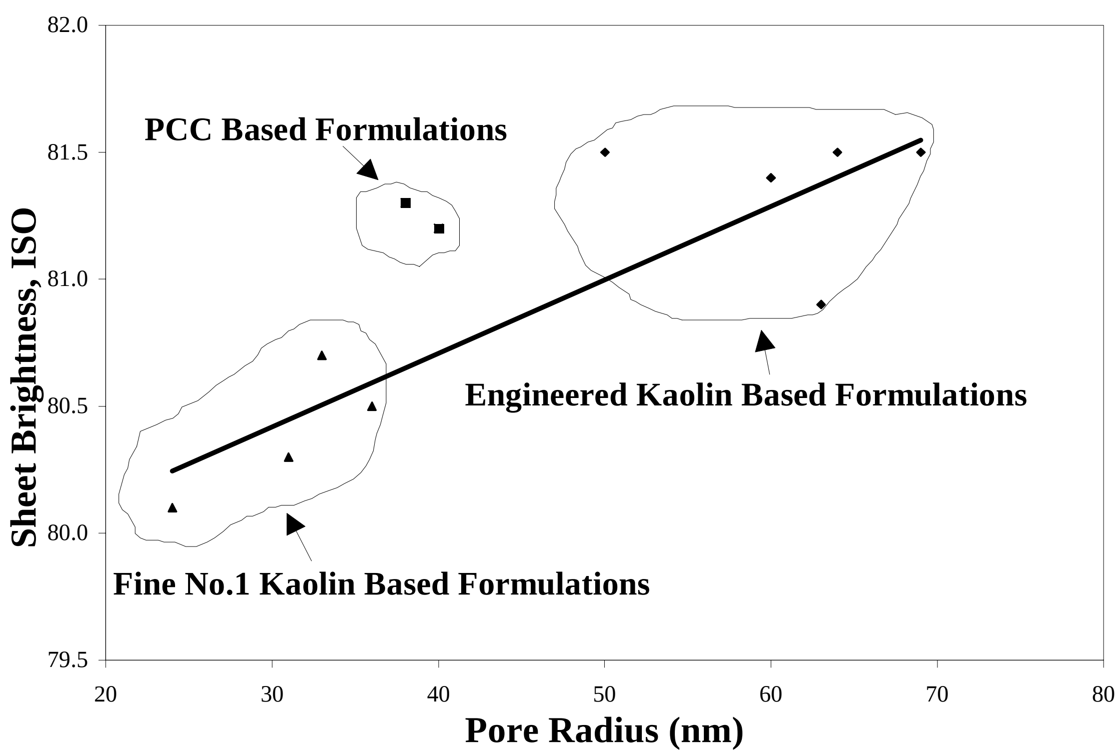

Figure 8. Sheet brightness influenced by coating structure.

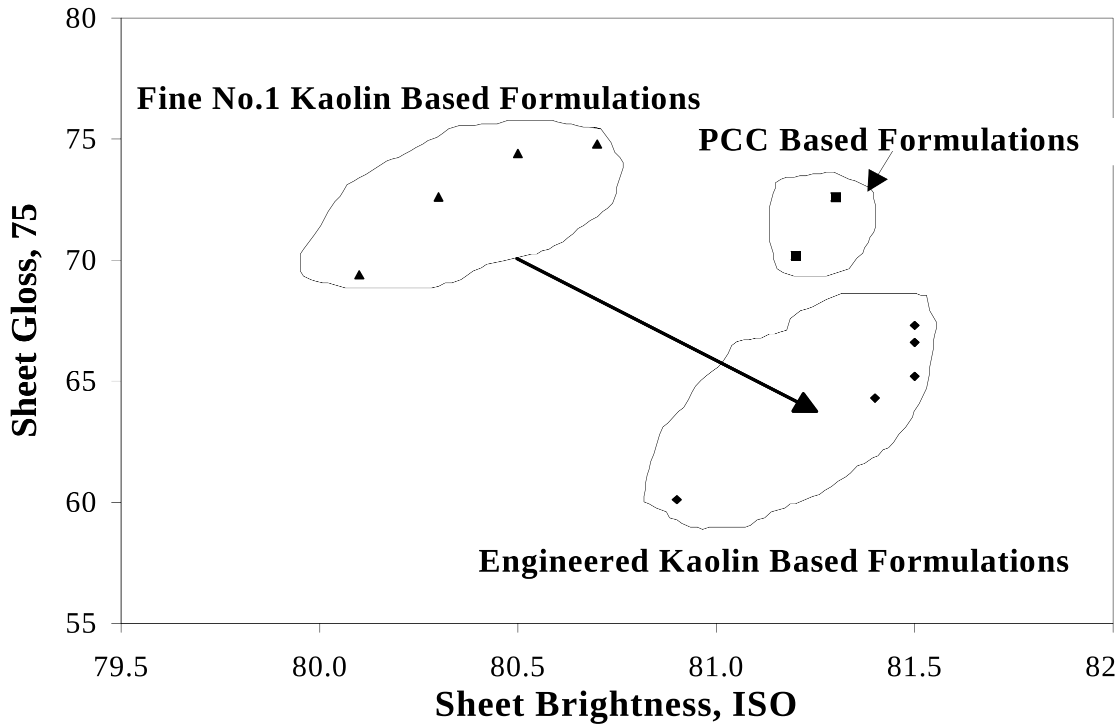

Figure 9. Sheet gloss versus sheet brightness.

In addition, when constant gloss calendering conditions are applied, an increased sheet brightness is expected for fine #1 kaolin based formulations in comparison to engineered kaolin. This is because the fine #1 kaolin glosses more easily than engineered kaolin.

Figure 10 shows that delta gloss correlates well to the pore radius. It was reported that a coating structure with bigger pores on the surface layer could allow slower ink set rate and hence longer ink leveling time for good delta gloss [8]. **Figures 11** through **14** show that there are a variety of other structural effects on sheet gloss, print gloss, delta gloss and delta goniophotometer peak width. The functions plotted in each graph are linear in each independent variable. Details of these regressions are provided in Appendix B. In Figure 11, sheet gloss can be seen to be influenced by macroscopic (Paperscape) and microscopic (AFM) topography. These parameters determine the angular spread of the glossmeter light beam reflected off the surface. Print gloss, in Figure 12, is influenced by sheet gloss, pore radius and microscopic roughness. It is common knowledge that sheet gloss strongly affects print gloss. The fact that microscopic roughness affects print gloss independently of sheet gloss means this parameter affects sheet and print gloss through different mechanisms. While microscopic roughness affects sheet gloss by spreading the glossmeter beam, it may affect print gloss through the ability of the ink layer to hide it. Print gloss is also affected by pore radius, possibly through the effects of pore radius on capillary imbibition forces. Larger pore radii yield lower capillary forces, usually reducing ink imbibition and setting rates. It is hypothesized that ink imbibition may affect the index of refraction of the printed paper surface, while reduced setting rates may allow greater leveling of ink film split patterns. Delta gloss can be seen, in Figure 13, to depend upon the same structural parameters as print gloss. The quality of the empirical functional fits is remarkable. Essentially all of the variation in both print gloss and delta gloss is explained by these structure parameters. There is a notable absence of any effect of surface void volume, as measured via polarized goniophotometry, upon print gloss or delta gloss.

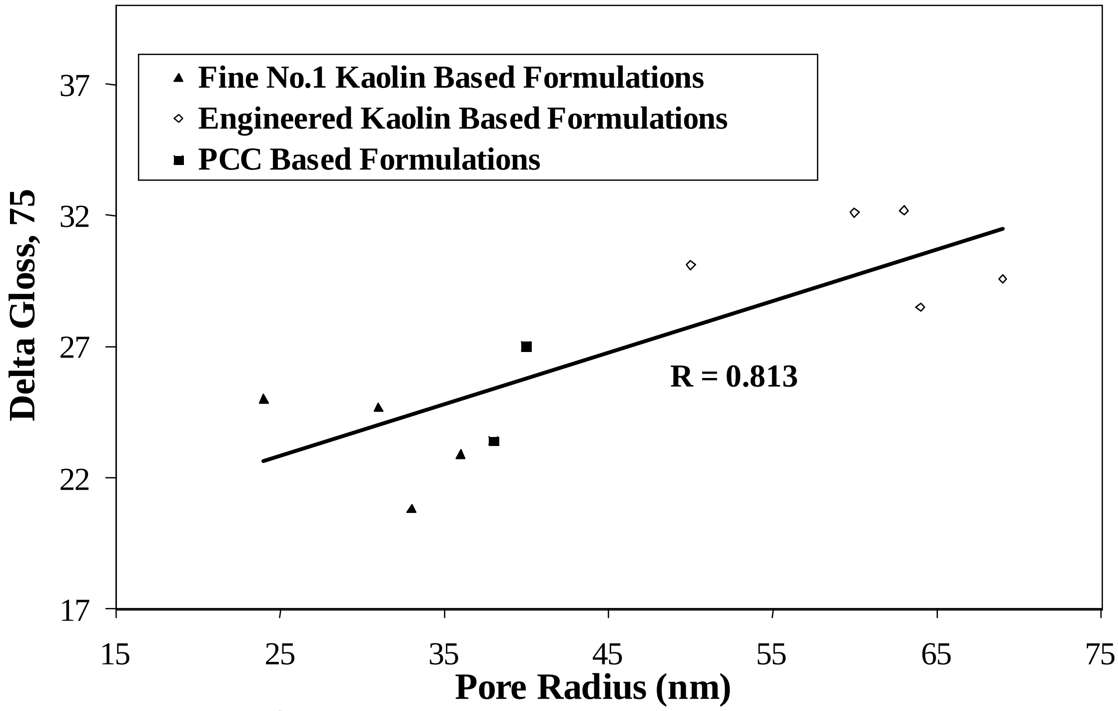

Figure 10. Delta gloss influenced by pore size.

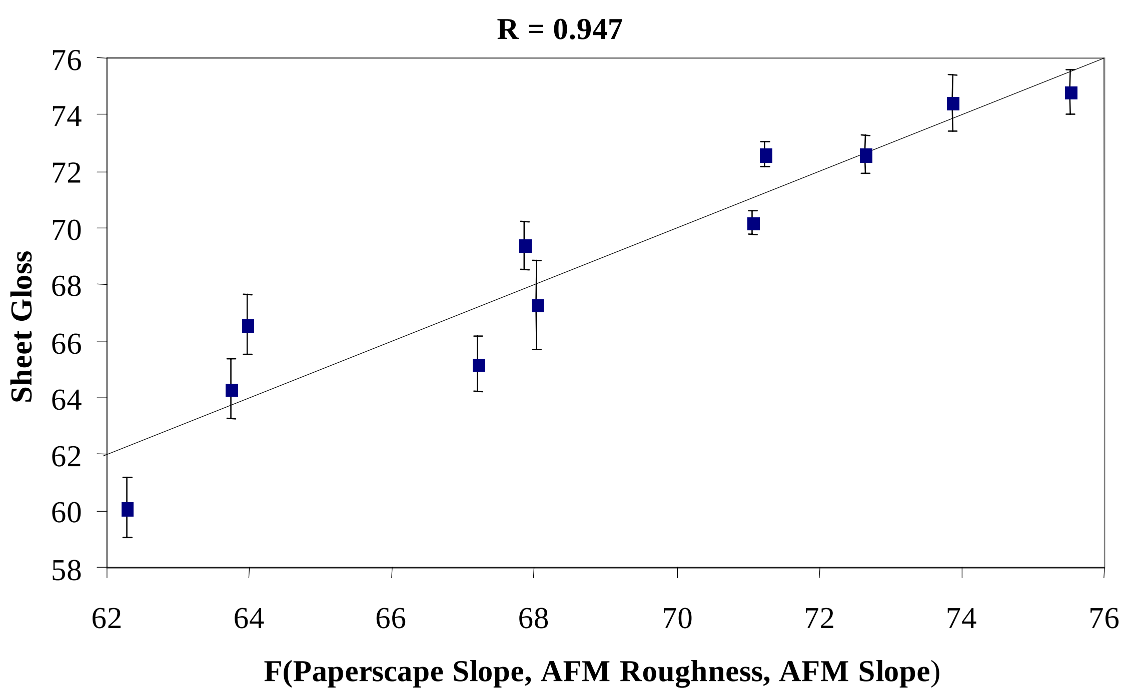

Figure 11. Sheet gloss dependence on structural parameters.

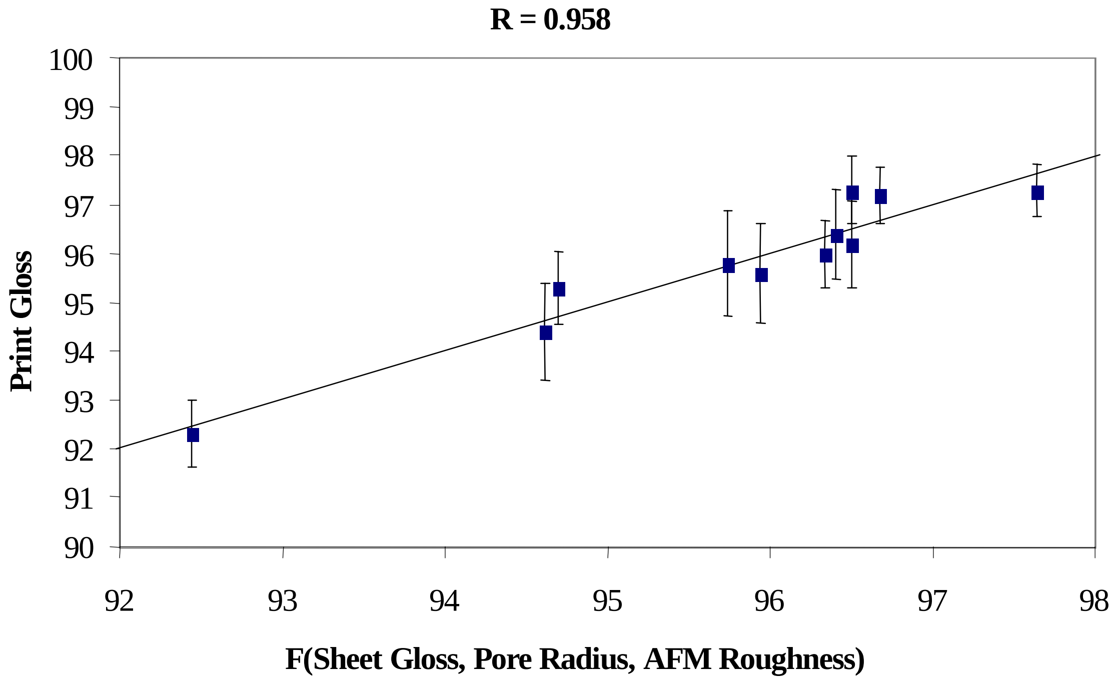

Figure 12. Print gloss dependence upon structural parameters.

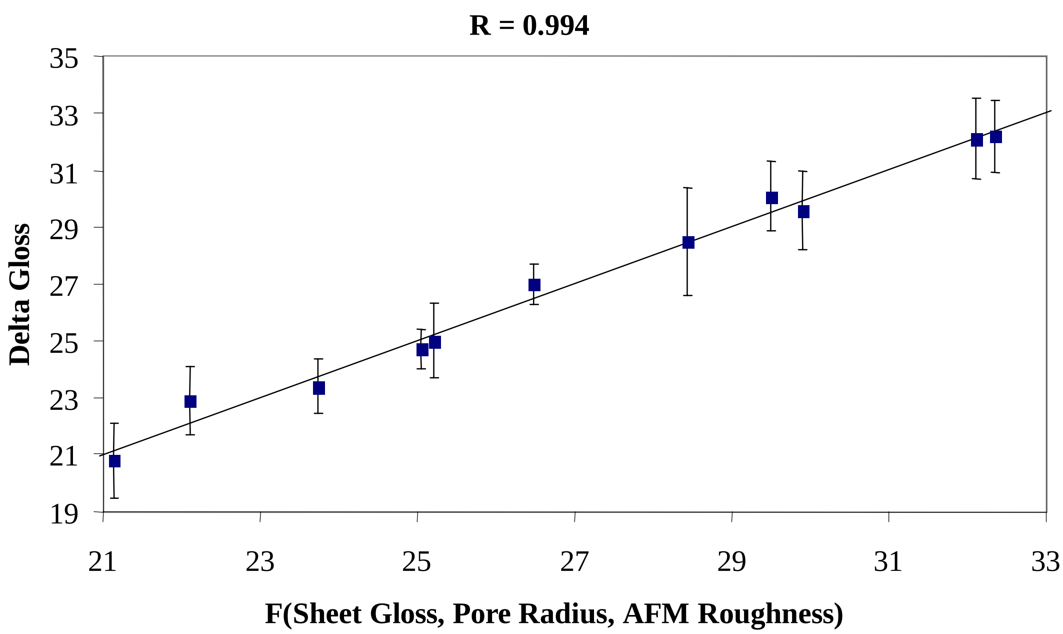

Figure 13. Delta gloss dependence upon structural parameters.

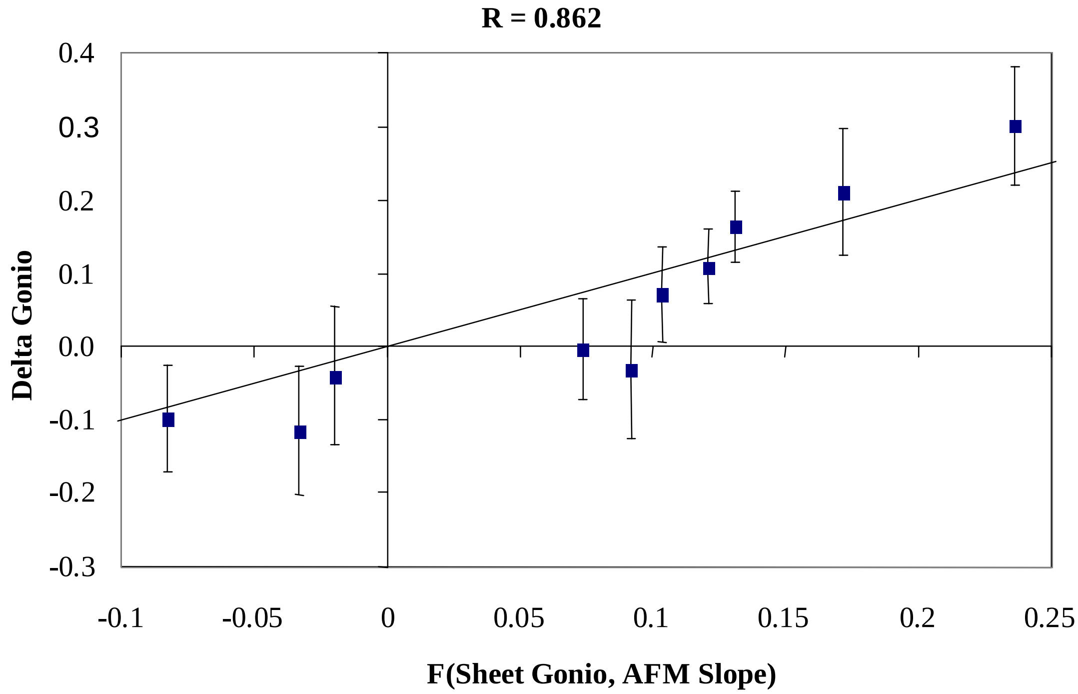

Figure 14. Delta goniophotometry dependence upon structural parameters.

Remembering Figure 3, there were gross differences in the changes in gloss measurements and goniophotometry upon printing. An examination of Figure 14 shows that the change in goniophotometer peak width depends upon a different set of structural parameters than does delta gloss. Both delta gloss and goniophotometer delta peak width depend on the sheet values for these measurements. Both deltas also depend on atomic force microscope scale topographical parameters. However, delta gloss has a dependence on pore radius while the goniophotometer delta does not. It is known that gloss measurements are influenced by the index of refraction of a surface whereas goniophotometer peak width measurements are not. Thus it is hypothesized that the influence of pore radius is related to ink imbibition, which may be affecting the index of refraction of the printed paper surface. However, this hypothesis has not been tested and may be proven or refuted through future measurements.

Figure 15 shows the ink on paper tack development with time for two kaolin/PCC formulations. In Figure 15(a), "Fine No.1 Kaolin/PCC A" & "Engineered Kaolin/PCC A" refer to coatings C & I, respectively. And in Figure 15(b), "Fine No.1 Kaolin/PCC B" & "Engineered Kaolin/PCC B" refer to coatings D & J, respectively. It is clear that the initial separation force of the fine #1 kaolin based coating is greater than that of the engineered kaolin based coating. The higher the initial slopes of the separation force curve the faster the ink set rate is. Engineered kaolin gives a slower ink set rate compared to fine #1 kaolin when the same amounts of carbonates are used in the formulations. This is consistent with the trend to higher delta gloss for engineered kaolin shown in Figure 10.

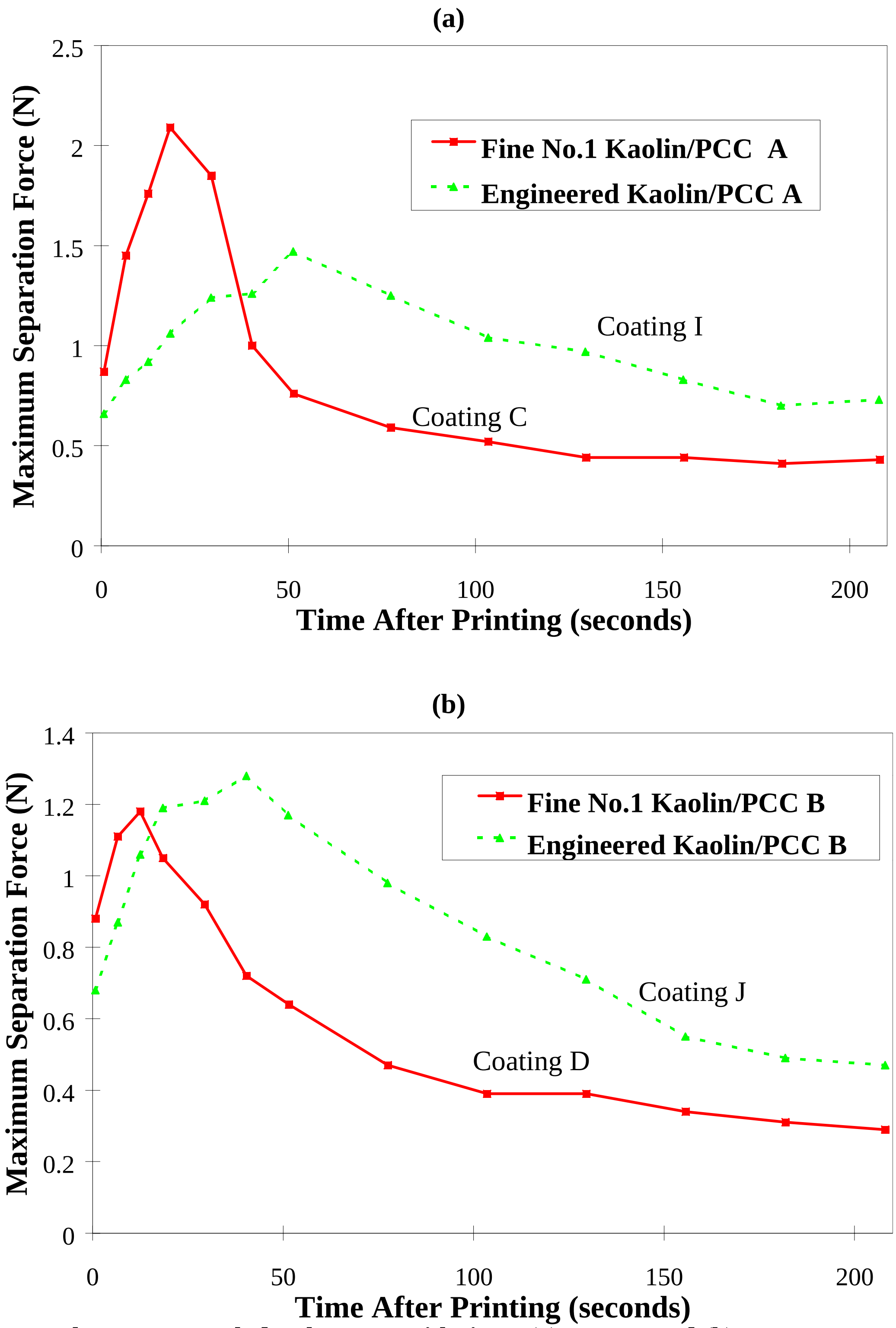

Figure 15. Ink on paper tack development with time: (a) PCC A and (b) PCC B.

It is also noticed that, upon reaching its peak value, the separation force drops almost instantly for fine #1 kaolin/PCC B. In contrast, there is a plateau for the formulation using engineered kaolin/PCC B. The pore volume for fine #1 and engineered kaolins used with coating PCCs is given in **Figure 16**. It appears that the high pore volume associated with fine #1 kaolin could also be responsible for accelerating the ink set rate and thus giving a low delta gloss. **Figure 17** shows that K&N ink receptivity is also influenced by coating structure, in particular the pore radius. A low K&N is an indication of a less porous coating structure and a potential problem with glueability. **Figure 18** is a plot of IGT pick strength versus pore size. The highest pick strengths are obtained for the coatings with the largest pore sizes. Large pores are associated with engineered pigments, with relatively few fine particles. The reduction in the number of fine particles typically reduces surface area, which is well known to influence binder demand and pick strength.

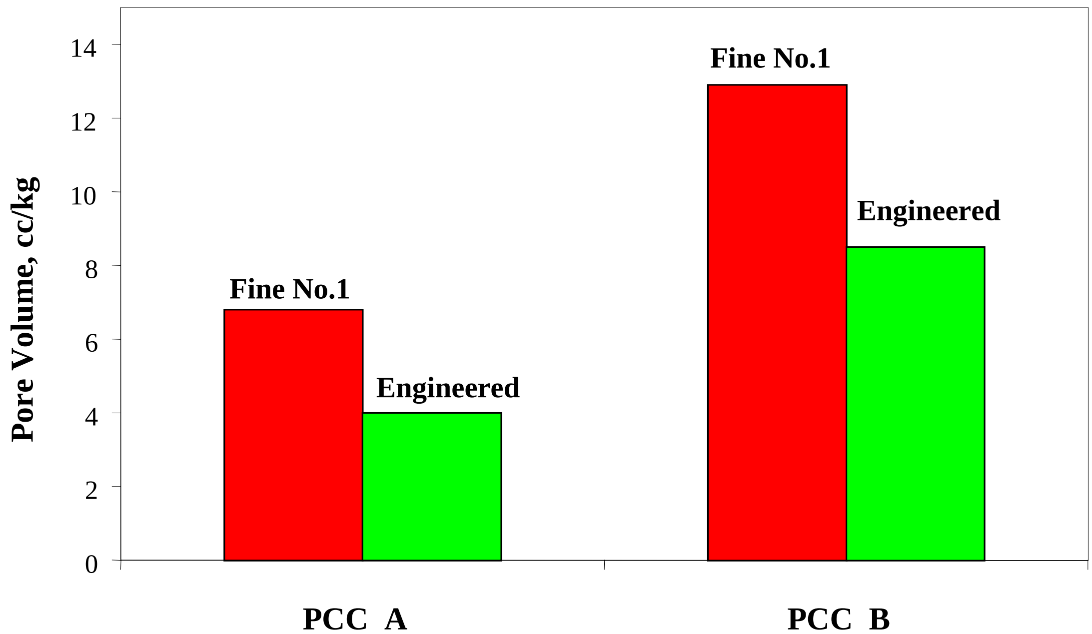

Figure 16. Pore volume for fine no. 1 or engineered kaolins based formulations.

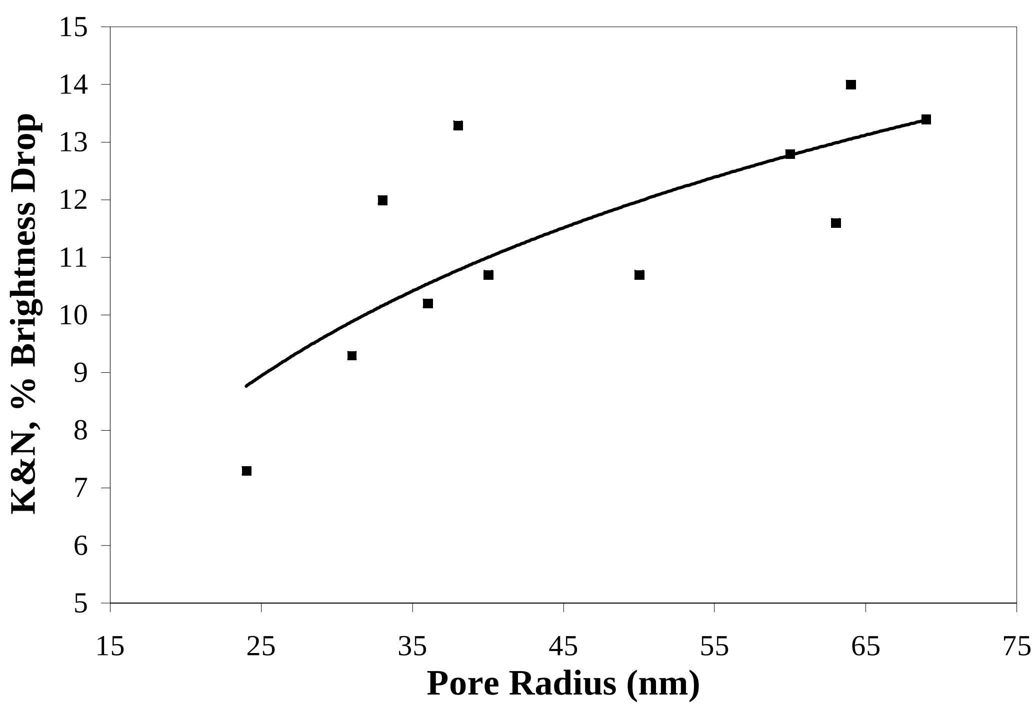

Figure 17. K&N ink receptivity influenced by coating structure.

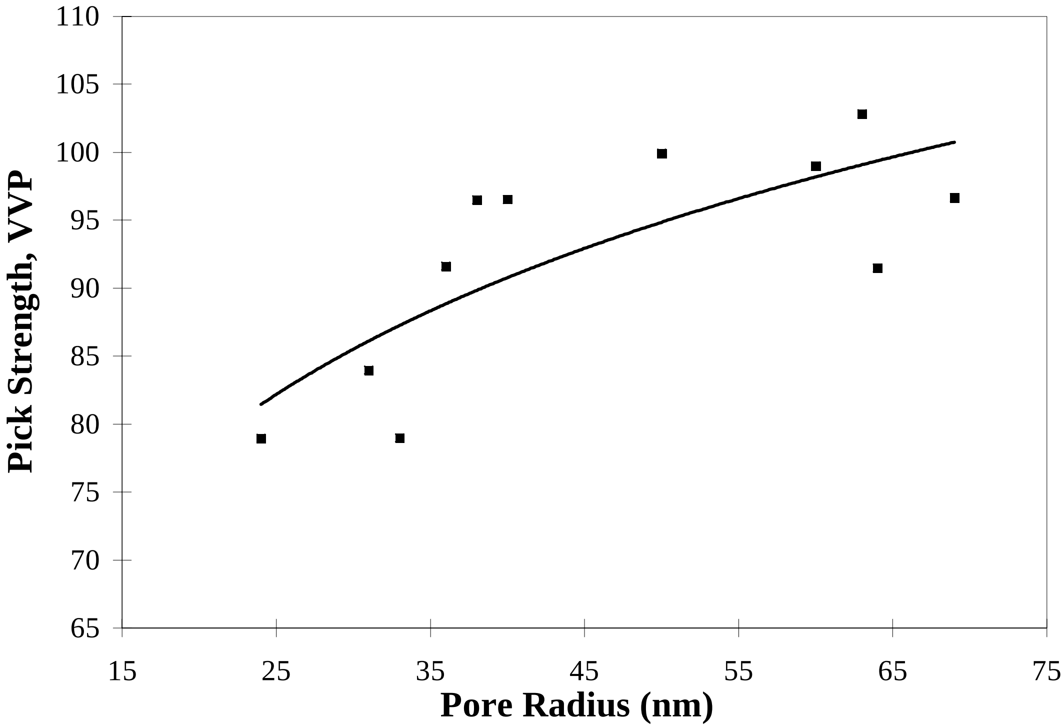

Figure 18. Pick strength versus pore size.

CONCLUSIONS

It has been shown that the coating structure can be related to the sheet properties of coated paper for both high clay (engineered/fine #1 kaolins) and high carbonate (coating PCCs/GCCs) based formulation systems. Sheet brightness, which is very critical for coated freesheet and woodfree grades as well as for coated SBS, depends strongly on the pore radius of coatings. Engineered kaolins create a coating structure with relatively larger pore radii, and thus provide better light scatter than fine #1 kaolins. Fine #1 "glossing" kaolins can, however, allow higher carbonate loading in the formulations for increased light scatter and decreased optical absorption, and hence provide much improved sheet brightness while meeting sheet gloss targets. Coating PCCs can give higher sheet brightness compared to the use of the glossing GCCs, due primarily to their light scattering ability, which is in turn related to the particle morphology, mean particle size and particle size distribution. Among the coating PCCs, the one giving larger coating pore volumes yielded higher sheet brightness.

Sheet gloss has been correlated to macroscopic and microscopic surface topography. Surfaces with greater roughness and higher slopes will spread the reflected glossmeter beam to a greater extent, thus reducing gloss. Fine #1 kaolins together with coating PCCs provide excellent sheet gloss.

Delta gloss and print gloss are influenced by sheet gloss, pore radius and microscopic roughness. Pore radius could possibly affect print and delta gloss through capillary imbibition forces. The effect of pore volume is also important. There can be more uncertainty in the measurement of pore volume mainly due to the influence of coat weight. However, it is believed that a coating structure with smaller pores but a larger pore volume can facilitate ink set rate (typically with higher slope or a smaller integral in the ink tack build curve) and hence give a short ink leveling time to yield a lower delta gloss. Engineered kaolins (or high carbonate) based formulations therefore have advantages in this regard.

Structural parameter analysis has revealed that the change of the goniophotometer peak width upon printing is affected by the microscopic slope as well as by the goniophotometer peak width of the unprinted sheet. It is interesting that the goniophotometer delta is not influenced by pore radius, which does affect the delta gloss. It is therefore hypothesized, subject to future proof, that capillary imbibition of ink may affect the index of refraction of a printed paper surface. Changing the index of refraction may in turn affect delta gloss, but should not affect measurements made using goniophotometry.

Coating structure will influence strength properties of a coated surface. Of high importance in topcoat applications are IGT dry pick strength of the surface in all applications and glueability of the surface in coated paperboard applications. The highest pick strengths of the coatings studied are associated with the engineered pigments, which have reduced fine particle content. A finer particle is well known to increase surface area and thus binder demand. K&N ink receptivity is an indicative parameter of the resistance to print mottle and the glueability characteristics of a coated sheet. Coatings with larger pore radii generally have better K & N ink receptivity, reduced print mottle and improved pick strength.

Overall, engineered kaolins, in combination with engineered ground or precipitated carbonates, provide significant opportunities to improve brightness, sheet and print gloss, shade, and pick strength in high kaolin-based formulations. For high carbonate systems (Figure 9), we have found kaolin and carbonate combinations that give synergistic effects that allow improvements both in sheet gloss and sheet brightness. This is an attractive option for coated freesheet and woodfree mills that pursue a high brightness grade while maintaining other sheet properties with a potentially reduced production cost. The increased coverage and bulk that is provided by these structured coatings could also lend themselves to the production of lower basis weight, higher brightness publication grades. Alkaline coated SBS producers can also take advantage of these concepts to produce bluer and whiter grades while maintaining their other sheet properties along with gaining a cost advantage.

ACKNOWLEDGMENT

The authors would like to thank the technicians in Sandersville's Paper Technology Development Department of the IMERYS Pigments and Additives Group for their efforts in paper coating, testing and analysis of the physics influencing the results of this work. The authors would also like to thank Dr. Frank A. Adamsky for his input in developing the market needs for coated board applications for us.

REFERENCES

1. Climpson, N. A. and Taylor, J. H., “Pore Size Distribution and optical scattering coefficients of clay structures”, *Tappi J.*, **59**(7): 89 (1976).

2. Abrams, L., Capano, P. J., Favorite, C. W., Johnson, R. W., "Using Mercury Porosimetry to Characterize Coating Pore Structure and Its Relation to Coating Optical Performance," 1996 TAPPI Coating Conference Proceedings, p. 185.
3. Johnson, R. W., Abrams, L., Maynard, R.B. and Amick, T. J., "Use of Hg Porosimetry to Characterize Pore Structure and Model End-use Properties of Coated Papers", Part I. Optical and Strength Properties, 1998 Coating Conference Proceedings, p. 337.
4. Wygant, R. W., Pruett, R. J. and Chen, C.-Y., "A Review of Techniques for Characterizing Paper Coating Surfaces, Structures and Printability," 1995 TAPPI Coating Fundamentals Symposium Proceedings, p. 1.
5. Wygant, R. W., Iyer, R. R., Jones, J. P. E, and Cummings, D. O., "Glossing Properties of Engineered Kaolins," 1998 TAPPI Coating Conference Proceedings, p. 837.
6. Gate, L. F. and Leaity, K, "New Aspects on the Gloss of Coated Paper," TAPPI 1991 Coating Conference Proceedings, p. 473.
7. Gane, P. A. C., Seyler, E. N., "Tack Development: An Analysis of Ink/Paper Interaction In Offset Printing", 1994 TAPPI Coating Conference Proceedings, p. 243.
8. Arai, Y. and Nojima, K., "Coating Structure For Obtaining High Print Gloss", 1997 TAPPI Coating Conference Proceedings, p. 133.

Received: February 25, 2000
Accepted: September 19, 2000

This paper was accepted for abstracting and publication in the March 2001 issue of *TAPPI JOURNAL*.

TAPPI Website: www.tappi.org

APPENDIX A Pigment, Binder and Additive Identities

Pigments	Kaolin A - High Brightness Ultrafine #1 Kaolin
	Kaolin B - Engineered Kaolin
	GCC A - Fine Ground Calcium Carbonate
	GCC B - Engineered Ground Calcium Carbonate
	GCC C - Ultrafine Ground Calcium Carbonate
	PCC A - Fine Precipitated Calcium Carbonate
	PCC B - Ultrafine Precipitated Calcium Carbonate
Binders	Latex - BASF styrene acrylic copolymer
	Protein - Protein Technologies Procote 2500
Additives	0.5 part Nopcote C-104 - calcium stearate lubricant
	0.1 part Allied Colloids Dispex - sodium polyacrylate dispersant

APPENDIX B Multi-Linear Regression Analyses

The regressions shown in Figures 11 through 14 of the main text are described in this appendix. These regressions are all linear in each of the independent variables. Such regressions were found for most final sheet properties as functions of those properties, which may be thought of as describing the structure of the coating layers. These structural properties included topographical statistics derived from atomic force microscope (AFM) and ECC Paperscape (a stylus profilometer) scans, Parker Print-Surf S10 roughness, coating layer pore size and volume measurements obtained from mercury porosimetry and effective index of refraction measurements obtained through polarized light goniophotometry. Of these, only AFM RMS roughness and slope, Paperscape slope, and mercury porosimeter pore size data were found to influence final sheet properties. Only gloss properties, including sheet gloss, print gloss, delta gloss and delta goniophotometer peak width (where delta refers to the change upon printing) were found to be well predicted by the structural properties.

Table B1 below provides some details of the regression results. These include the independent variables included in each fit, the coefficient and significance of each independent variable, the range of each independent variable and the total variation in the regression function resulting from the range of variation of each variable.

The regression for sheet gloss shows dependencies on AFM roughness and slope and Paperscape slope. However, it should be noted that the dependence on Paperscape slope is of low significance. This has been included merely to illustrate the affects of topography on sheet gloss at both microscopic and macroscopic length scales. All other structural properties had much lower influences. Interestingly, AFM roughness and AFM slope have coefficients of opposite sign and provide variation in the regression function of nearly equal and opposite amount. The range in Paperscape slope values provides much less variation in the regression function. It is intuitively obvious that increasing AFM roughness should decrease gloss. However, it appears highly counterintuitive that gloss would increase with increasing AFM slope. The explanation for this lies in the fact that AFM roughness and slope are not truly independent of each other. In fact, slope should be related to the ratio of roughness to lateral feature size. At equal lateral features sizes, higher roughnesses will yield higher slopes. **Table B2** below shows that there is a moderately strong positive correlation between AFM roughness and AFM slope, whereas neither of these correlates well to the Paperscape slope. Thus, although somewhat interdependent, AFM slope and roughness both contribute simultaneously and significantly to the regression fit.

The regression results for print gloss and delta gloss are very similar. Both depend significantly on AFM roughness, pore radius and sheet gloss. In both regressions AFM roughness has the greatest influence, whereas pore radius and sheet gloss reverse rankings in the two regressions. Once again, counterintuitive results are shown, with increasing AFM roughness apparently increasing both print gloss and delta gloss and larger pore radii decreasing both print and delta gloss. However, the same variable interdependence argument used above can again be invoked in explanation. **Table B3** shows the correlations between the supposedly independent variables used in these regressions. Sheet gloss correlates moderately well, and negatively, to both AFM roughness and pore radius, while there is a strong positive correlation between AFM roughness and pore radius. It should also be remembered that sheet gloss was found to be most strongly influenced by AFM roughness. The fact that AFM roughness has the strongest influence on all three gloss measurements, while print and delta gloss also depend on sheet gloss, indicates that AFM roughness has a different mode of influence on print and delta gloss than on sheet gloss. An examination of the signs of coefficients in Table B1 may help to understand this. Increasing AFM roughness decreases sheet gloss. Increasing sheet gloss increases print gloss, but decreases delta gloss. From this, it is not immediately obvious what the net affect of AFM roughness on print gloss is. However, it is clear that increasing AFM roughness actually increases delta gloss. A hypothetical physical mechanism for this might be that printed ink layers may be able to hide roughness on the microscopic scale of AFM measurements. For two sheets of similar sheet gloss, the sheet with greater microscopic roughness (and lower macroscopic roughness) may have greater delta gloss than the sheet with lower microscopic roughness (and greater macroscopic roughness). This is due to the thin ink layer being better able to hide the microscopic roughness than the macroscopic roughness. The negative coefficient for pore radius is also an 'artifact' of the multiple not-quite-independent variable regression, as it is clearly seen in Figure 10 of the main text that, considered in isolation, increasing pore radius does increase delta gloss.

The regression for delta goniophotometer peak width shows dependencies on both sheet goniophotometer peak width and AFM slope. Unpublished regressions for sheet and print goniophotometer peak widths do not show significant dependencies on AFM slope, and **Table B4** shows little correlation between AFM slope and sheet goniophotometer peak width. The negative sign of the coefficient for sheet gonio in Table B1 perhaps indicates that sheets with low peak width will have less peak width decrease upon printing, i.e., smoother sheets will be smoothed less. The positive sign of the coefficient for AFM slope may again relate to the thin ink layer being better able to hide AFM scale topographical features.

Dependent Variable	Independent Variable	Independent Variable Coefficient	Independent Variable Significance	Independent Variable Range	Regression Function Variation
Sheet Gloss	AFM Roughness	-284	0.000	0.028	-8.06
	AFM Slope	1.03	0.004	7.48	7.69
	Paperscape Slope	-1.25	0.241	0.22	-0.28
Print Gloss	AFM Roughness	132	0.001	0.028	3.76
	Pore Radius	-0.07	0.028	26	-1.92
	Sheet Gloss	0.42	0.000	4.2	1.76
Delta Gloss	AFM Roughness	132	0.001	0.028	3.76
	Sheet Gloss	-0.58	0.028	4.2	-2.44
	Pore Radius	-0.07	0.000	26	-1.92
Delta Gonio	Sheet Gonio	-0.70	0.028	0.45	-0.31
	AFM Slope	0.02	0.002	7.48	0.18

Table B1. Details of the multi-linear regressions.

	Paperscape Slope	AFM Roughness
AFM Roughness	0.09	
AFM Slope	-0.04	0.59

Table B2. Cross correlations between structural properties that influence sheet gloss.

	Sheet Gloss	Pore Radius
Pore Radius	-0.76	
AFM Roughness	-0.77	0.92

Table B3. Cross correlations between structural properties that influence print and delta gloss.

	Sheet Gonio
AFM Slope	0.28

Table B4. Cross correlations between structural properties that influence delta goniophotometer peak width.